Postprint of: Kozieł S., Sigurdsson A., Triangulation-based Constrained Surrogate Modeling of Antennas, IEEE TRANSACTIONS ON ANTENNAS AND PROPAGATION, Vol. 66, iss. 8 (2018), pp. 4170-4179, DOI: 10.1109/TAP.2018.2839759

© 2018 IEEE. Personal use of this material is permitted. Permission from IEEE must be obtained for all other uses, in any current or future media, including reprinting/republishing this material for advertising or promotional purposes, creating new collective works, for resale or redistribution to servers or lists, or reuse of any copyrighted component of this work in other works.

Triangulation-based Constrained Surrogate Modeling of Antennas

Slawomir Koziel, *Senior Member*, *IEEE*, and Ari T. Sigurðsson

***Abstract*—Design of contemporary antenna structures is heavily based on full-wave electromagnetic (EM) simulation tools. They provide accuracy but are CPU-intensive. Reduction of EM-driven design procedure cost can be achieved by using fast replacement models (surrogates). Unfortunately, standard modeling techniques are unable to ensure sufficient predictive power for real-world antenna structures (multiple parameters, wide parameter ranges, highly-nonlinear responses). Here, a design-oriented modeling technique is introduced, in which the most critical part is the domain definition. The surrogate is constructed in the region based on a set of reference designs, optimized with respect to user-selected figures of interest such as operating frequencies, bandwidth, substrate permittivity, etc. The domain is spanned by the simplexes, obtained by triangulation of the reference designs, further extended into their orthogonal complements. Restricting the model domain as above permits dramatic reduction of the number of training data samples necessary to build a reliable model, as compared to the conventional approach. The proposed modeling framework is demonstrated using three examples, a UWB monopole, and two dual-band antennas. Comprehensive benchmarking as well as application studies and experimental verification are also provided.**

***Index Terms*—Antenna design, surrogate modeling, approximation models, simulation-driven design, constrained modeling, triangulation.**

I. Introduction

Perhaps the most fundamental tool in the design of contemporary antenna structures is full-wave electromagnetic (EM) simulation. On one hand, EM-driven design is compulsory as it is the only way to ensure reliability of the design process. This is especially the case for complex structures with large number of geometry parameters and/or when various interactions have to be accounted for (presence of housing, radomes, connectors, etc.). On the other hand, high-fidelity EM analysis tends to be computationally expensive, which poses some practical difficulties. In particular, design optimization of multiple antenna dimensions may become prohibitive when using conventional numerical algorithms. This issue might be partially alleviated by means of interactive approaches such as supervised parameter sweeping where the human factor (engineering experience) typically brings down the design time to acceptable levels. In practice, only the most important antenna parameters can be handled this way and, therefore, sub-optimal designs are obtained. As mentioned before, automated numerical optimization is most often impractical when using conventional algorithms [1], [2], particularly population-based metaheuristics [3], [4], due to their tremendous computational complexity. A practical approach to speeding up the optimization process is the use of adjoint sensitivities [5]-[7], which is, unfortunately, limited by commercial availability of adjoint technology (currently, CST [8] and HFSS [9]). Other approaches, which have been attracting considerable attention in recent years, are surrogate-assisted methods [10]-[13] (space mapping [11], response correction techniques [12], feature-based optimization [13]), where direct optimization of the expensive EM model is replaced by iterative construction and re-optimization of its cheaper representation (surrogate).

Clearly, design closure is not the only type of EM-driven task that incurs considerable computational expenses. Other common design procedures include re-design of an antenna for different operating conditions (operating frequency, bandwidth), various material parameters (substrate permittivity, substrate thickness), statistical analysis (e.g., yield estimation [14]), as well as robust design (e.g., optimization accounting for manufacturing tolerances [15], design centering [16]). All of these tasks involve a large number of structure evaluations, the cost of which can be prohibitive when performed directly using an EM solver.

Utilization of fast replacement models (surrogates) permits considerable computational savings. Among various modeling approaches, approximation-based surrogates (also referred to as data-driven models) are by far the most popular [17]. The underlying concept is approximation of sampled EM simulation data using kriging [18], radial basis function interpolation [18], neural networks [19], Gaussian process regression [20], support vector regression [21], [22], or polynomial regression [23], although that last technique is mostly suitable for local modeling. The principal advantage of data driven models is their low evaluation cost. The disadvantage is high cost of training data acquisition. In particular, the number of samples required to ensure acceptable accuracy (typically, relative RMS error at the level of 5 percent or less [24]) grows very quickly with the dimensionality of the design space (so-called curse of dimensionality) as well as (or even faster) with the parameter

The manuscript was submitted on September 22, 2017. This work was supported in part by the Icelandic Centre for Research (RANNIS) Grant 174114051, and by National Science Centre of Poland Grant 2015/17/B/ST6/01857.

S. Koziel and A.T. Sigurðsson are with Engineering Optimization and Modeling Center of Reykjavik University, Reykjavik, Iceland (e-mails: koziel@ru.is, aris14@ru.is); S. Koziel is also with Faculty of Electronics, Telecommunications and Informatics, Gdansk University of Technology, 80-233 Gdansk, Poland.

0018-926X (c) 2018 IEEE. Personal use is permitted, but republication/redistribution requires IEEE permission. See http://www.ieee.org/publications_standards/publications/rights/index.html for more information.

This article has been accepted for publication in a future issue of this journal, but has not been fully edited. Content may change prior to final publication. Citation information: DOI 10.1109/TAP.2018.2839759, IEEE Transactions on Antennas and Propagation

ranges. The latter need to be wide in order to cover decent range of operating conditions and/or material parameters. Due to the aforementioned issues, standard approximation models can only be used in low-dimensional parameter spaces (up to 5-6 dimensions) and for relatively narrow parameter ranges.

A constrained sampling technique has been introduced in [25] as an attempt to reduce the number of training data points necessary to construct the surrogate model. The principal concept behind [25] was to limit the model domain to a vicinity of a polygon spanned by the reference designs optimized for a range of operating conditions, in particular, the operating frequency of the antenna at hand. Further development of this idea was presented in [26] by extending it to two-dimensional space of figures of interest (specifically, the operating frequency and substrate permittivity). A downside of the technique of [26] is that a particular number of the reference designs and their particular arrangement (rectangular grid) is required. Obviously, this limits a range of practical applications of the technique as it does not allow for reusing pre-existing (optimized) designs.

In this work, we propose a generalized framework for design-oriented constrained modeling of antenna structures. The framework is a significant extension of [26]. In our methodology, a surrogate model domain is determined with respect to a set of reference designs that can be optimized with respect to any number of figures of interest and/or material parameters and can be allocated in an arbitrary manner. The reference designs can also be any designs that are already available for a given antenna structure (e.g., those obtained for other sets of performance specifications). The reference designs are subjected to Delaunay triangulation and the resulting simplexes are utilized to determine the model region of validity by extending them in orthogonal directions using a user-defined "thickness" parameter. The proposed technique is demonstrated using three examples: a UWB monopole and two dual-band antennas. Comprehensive benchmarking using kriging interpolation in an unconstrained domain indicate significant reduction of the number of samples necessary to establish models of comparable accuracy. Furthermore, application studies are provided along with experimental validation.

II. Triangulation-Based Constrained Modeling

In this section, the proposed modeling methodology is introduced. Its foundation is to define the surrogate model domain based on a set of simplexes spanned by triangulated reference designs that are optimized with respect to selected figures of interest such as operating conditions, material parameters, etc. This allows for focusing only on the part of the parameter space that contains "good" designs (from the point of view of selected figures of merit). Consequently, considerable reduction of the number of training samples necessary to construct a reliable surrogate can be achieved.

A. Reference Designs and Triangulation

We use the symbols F_k, $k = 1, \ldots, N$, to denote the figures of interest that are to be considered in the design process. Typical examples include an operating frequency of the antenna (or frequencies in case of multi-band antennas), –10 dB bandwidth, relative permittivity or height of the substrate material (for a microstrip antenna), etc. The surrogate model will be constructed in the region spanned by the reference designs $\boldsymbol{x}^{(j)}$, $j = 1, \ldots, p$, that are optimized for selected values of the figures of interest $\boldsymbol{F}^{(j)} = [F_1^{(j)} \ldots F_N^{(j)}]$. The reference designs can be obtained specifically for the purpose of building the model or be available beforehand (e.g., from previous design cases of a structure at hand). The latter is of particular interest because it allows us to reuse already existing designs. Also, it should be noted that the reference designs do not have to be exactly optimal because the surrogate model domain is spanned by these designs but it is not restricted to them (as explained later, they are allocated in the domain interior).

Given the reference designs, a set of simplexes is created as elementary cells utilized in the model domain definition. Assignment of the reference designs to the simplexes is realized using Delaunay triangulation [27] which ensures possibly largest angles between the simplex vertices. The sets of vertices of the simplex $S^{(k)}$, $k = 1, \ldots, N_S$, is denoted as $S^{(k)} = \{\boldsymbol{x}^{(k.1)}, \ldots, \boldsymbol{x}^{(k.N+1)}\}$, in which $\boldsymbol{x}^{(k.j)} \in \{\boldsymbol{x}^{(1)}, \ldots, \boldsymbol{x}^{(N)}\}$, $j = 1, \ldots, N + 1$, are individual vertices. In other words, the vertices $\boldsymbol{x}^{(k.j)}$ of the kth simplex are certain reference designs. A particular selection is an outcome of the triangulation process. The concept of reference designs, triangulation, and forming the simplexes has been shown in Fig. 1. In the example given, simplex $S^{(1)}$ is composed of the reference designs $\boldsymbol{x}^{(1)}$, $\boldsymbol{x}^{(2)}$, and $\boldsymbol{x}^{(4)}$, i.e., we have $\boldsymbol{x}^{(1.1)} = \boldsymbol{x}^{(1)}$, $\boldsymbol{x}^{(1.2)} = \boldsymbol{x}^{(2)}$, and $\boldsymbol{x}^{(1.3)} = \boldsymbol{x}^{(4)}$.

B. Surrogate Model Domain

In this section, a mathematical formalism is introduced that allows us to define the surrogate model domain X_S using the reference designs described in Section II.*A*. The domain is determined as a vicinity of the manifold M being the union of the simplexes $S^{(k)}$, i.e.,

$$M = \bigcup_k \{\boldsymbol{y} = \sum_{j=1}^{N+1} \alpha_j \boldsymbol{x}^{(k.j)} : 0 \le \alpha_j \le 1, \sum_{j=1}^{N+1} \alpha_j = 1\} \tag{1}$$

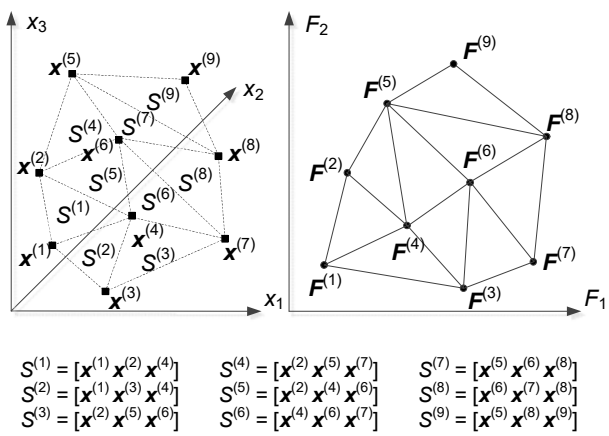

Fig. 1. Conceptual illustration of the reference designs and their triangulation. Reference designs in an example three-dimensional design space shown in the left panel; figures of interest vectors corresponding to the reference designs plotted in the two-dimensional feature space as well as their triangulation shown in the right panel. In the considered case, there are nine simplexes formed by the reference designs. In reference to the notation used in Section II.*A*, here, we have $N = 2$ (two figures of interest), $p = 9$ (nine reference designs), and $N_S = 9$ (nine simplexes).

MOST WIEDZY Downloaded from mostwiedzy.pl

026X (c) 2018 IEEE. Personal use is permitted, but republication/redistribution requires IEEE permission. See http://www.ieee.org/publications_standards/publications/rights/index.html for more information.

This article has been accepted for publication in a future issue of this journal, but has not been fully edited. Content may change prior to final publication. Citation information: DOI 10.1109/TAP.2018.2839759, IEEE Transactions on Antennas and Propagation

The vicinity is determined by the distance from M in the orthogonal complements of the subspaces (or hyper-planes) containing the simplexes $S^{(k)}$. In particular, in order to determine whether a given point $\boldsymbol{z}$ is within the model domain or not, one needs to find the distance between $\boldsymbol{z}$ and the manifold M in the sense highlighted above. In the remaining part of this section we give a rigorous definition of the domain X_S.

As a first step, let us consider a projection $P_k(\boldsymbol{z})$ of a point $\boldsymbol{z}$ onto the hyper-plane H_k containing the simplex $S^{(k)}$. The projection is defined as the point on the hyper-plane that is the closest to $\boldsymbol{z}$.

For convenience of notation, we define the simplex anchor $\boldsymbol{x}^{(0)} = \boldsymbol{x}^{(k.1)}$, and the spanning vectors $\boldsymbol{v}^{(j)} = \boldsymbol{x}^{(k.j+1)} - \boldsymbol{x}^{(0)}$, $j = 1, \ldots, N$. Explanation of these terms can be found in Fig. 2. The projection corresponds to the following expansion coefficients with respect to the vectors $\boldsymbol{v}^{(j)}$:

$$\arg \min_{[\bar{\alpha}^{(1)},\ldots,\bar{\alpha}^{(N)}]} \left\| \boldsymbol{z} - \left[\boldsymbol{x}^{(0)} + \sum_{j=1}^{N} \bar{\alpha}^{(j)} \bar{\boldsymbol{v}}^{(j)} \right] \right\|^2 \tag{2}$$

where the vectors $\bar{\boldsymbol{v}}^{(j)}$ are obtained from $\boldsymbol{v}^{(j)}$ by orthogonalization (i.e., $\bar{\boldsymbol{v}}^{(1)} = \boldsymbol{v}^{(1)}$, $\bar{\boldsymbol{v}}^{(2)} = \boldsymbol{v}^{(2)} - a_{12}\boldsymbol{v}^{(1)}$ where $a_{12} = \boldsymbol{v}^{(1)T}\boldsymbol{v}^{(2)}(\boldsymbol{v}^{(1)T}\boldsymbol{v}^{(1)}$, etc.). In general, we have

$$\bar{\boldsymbol{V}} = \left[\bar{\boldsymbol{v}}^{(1)} \ \bar{\boldsymbol{v}}^{(2)} \ \ldots \bar{\boldsymbol{v}}^{(N)} \right] = \left[\boldsymbol{v}^{(1)} \ \boldsymbol{v}^{(2)} \ \ldots \boldsymbol{v}^{(N)} \right] \boldsymbol{A} \tag{3}$$

where $\boldsymbol{A}$ is an upper-triangular matrix of coefficients obtained as a result of the above orthogonalization procedure.

The problem (2) is equivalent to

$$\left[\bar{\boldsymbol{v}}^{(1)} \ \bar{\boldsymbol{v}}^{(2)} \ \ldots \bar{\boldsymbol{v}}^{(N)} \right] \begin{bmatrix} \bar{\alpha}^{(1)} \\ \vdots \\ \bar{\alpha}^{(N)} \end{bmatrix} = \boldsymbol{z} - \boldsymbol{x}^{(0)} \tag{4}$$

Because the dimension of the simplex is normally lower than the dimension of the design space, the expansion coefficients can be found as follows

$$\begin{bmatrix} \bar{\alpha}^{(1)} \\ \vdots \\ \bar{\alpha}^{(N)} \end{bmatrix} = (\bar{\boldsymbol{V}}^T \bar{\boldsymbol{V}})^{-1} \bar{\boldsymbol{V}}^T (\boldsymbol{z} - \boldsymbol{x}^{(0)}) \tag{5}$$

In order to determine whether $P_k(\boldsymbol{z})$ is within the convex hull of the simplex $S^{(k)}$, one needs the expansion coefficients $\alpha^{(j)}$ of $\boldsymbol{z}$ with respect to the original vectors $\boldsymbol{v}^{(j)}$. These are given as

$$\begin{bmatrix} \alpha^{(1)} \\ \vdots \\ \alpha^{(N)} \end{bmatrix} = \boldsymbol{A} \begin{bmatrix} \bar{\alpha}^{(1)} \\ \vdots \\ \bar{\alpha}^{(N)} \end{bmatrix} \tag{6}$$

The projection $P_k(\boldsymbol{z}) \in S^{(k)}$ if and only if it is a convex combination of the vectors $\boldsymbol{v}^{(j)}$, i.e., if the following two conditions are satisfied:

1. $\alpha^{(j)} \geq 0$ for $j = 1, \ldots, N$, and
2. $\alpha^{(1)} + \ldots + \alpha^{(N)} \leq 1$.

In the next step we define $\boldsymbol{x}_{\max} = \max\{\boldsymbol{x}^{(k)}, k = 1, \ldots, p\}$ and $\boldsymbol{x}_{\min} = \min\{\boldsymbol{x}^{(k)}, k = 1, \ldots, p\}$. The vector $\boldsymbol{dx} = \boldsymbol{x}_{\max} - \boldsymbol{x}_{\min}$ determines the range of variation of antenna geometry parameters within M.

The domain X_S of the surrogate is defined similarly as in [26], by the following two conditions: a vector $\boldsymbol{y} \in X_S$ if and only if

1. The set $K(\boldsymbol{y}) = \{k \in \{1,\ldots,N_S\} : P_k(\boldsymbol{y}) \in S^{(k)}\}$ is not empty;
2. $\min\{\|(\boldsymbol{y} - P_k(\boldsymbol{y}))//\boldsymbol{dx}\|_\infty : k \in K(\boldsymbol{y})\} \leq d_{\max}$, where // denotes component-wise division, and $d_{\max}$ is a user-defined parameter.

The above conditions describe the following situation. First, the point $\boldsymbol{z}$ has to be sufficiently close to at least one of the simplexes in the "tangential" sense. Second, the point $\boldsymbol{z}$ has to be sufficiently close to at least one of the simplexes in the "orthogonal" sense. The distance here is measured as a fraction of vector $\boldsymbol{dx}$. Changing the value of $d_{\max}$ allows for convenient control of the (volume-wise) size of the surrogate model domain as compared to the size of the unconstrained design space. Particular values of $d_{\max}$ used in our numerical experiments are given in Section III. Graphical illustration of the meaning of the parameter $d_{\max}$ has been shown in Fig. 3.

A remark should be made on the number of reference designs needed. In general, more designs permit more precise definition of the surrogate model domain (in the sense of selecting only the relevant part of the design space). On the other hand, computational cost of identifying these designs (unless they are already available) calls for reducing the number. A rule of thumb would be to have at least as many designs as required to detect the model domain "curvature". Roughly speaking, this would correspond to a star distribution [31] supplemented by the corners of the region defined by the ranges of the figures of interest considered (so, three designs for one figure of interest, around nine designs for two figures, and fifteen for three figures). Still, any additional reference design gives extra information about appropriate allocation of the training samples.

By definition, we have $M \subset X_S$. Furthermore, given typical values of $d_{\max}$ of 0.1 to 0.2, the (volume-wise) size of X_S is significantly smaller than the hypercube defined by the vectors $\boldsymbol{x}_{\min}$ and $\boldsymbol{x}_{\max}$ (which would be used for training data sampling in conventional modeling). This is of fundamental importance because it allows for considerable reduction of the number of samples necessary for surrogate model construction.

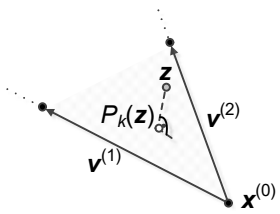

Fig. 2. Example simplex with its anchor and the spanning vectors as well as a point $\boldsymbol{z}$ and its projection onto the hyper-plane H_k containing $S^{(k)}$.

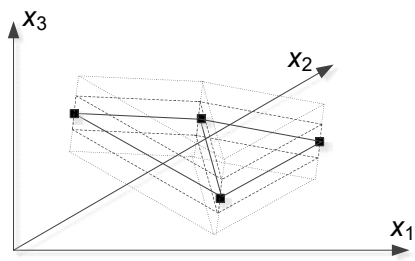

Fig. 3. Graphical illustration of the meaning of the thickness parameter $d_{\max}$ for a three-dimensional design space. Reference design marked with black squares, simplexes marked using solid lines. There are two surrogate model domains shown, corresponding to the smaller (dashed line) and larger (dotted line) values of $d_{\max}$. Small number of reference design shown for picture clarity.

MOST WIEDZY Downloaded from mostwiedzy.pl

0018-926X (c) 2018 IEEE. Personal use is permitted, but republication/redistribution requires IEEE permission. See http://www.ieee.org/publications_standards/publications/rights/index.html for more information.

This article has been accepted for publication in a future issue of this journal, but has not been fully edited. Content may change prior to final publication. Citation information: DOI 10.1109/TAP.2018.2839759, IEEE Transactions on Antennas and Propagation

At the same time, the set X_S contains the optimum designs for given sets of figures of interest, and, assuming sufficient regularity of the antenna responses w.r.t. its geometry parameters, optimum designs for all combinations of the same figures of interest within the convex hull of $\boldsymbol{F}^{(j)}$, $j = 1, \ldots, N$. This means that using a fraction of samples (required by the conventional model) it is possible to build a surrogate over a wide range of geometry/material parameters of the antenna as demonstrated in Section III.

C. Constructing Surrogate Model

Definition of the surrogate domain is the most important component of the modeling process. Having defined the domain, the training data is sampled within X_S, and the surrogate is constructed using kriging interpolation [18]. Real and imaginary parts of the reflection coefficients are modeled independently. For the convenience of the reader, a short summary of ordinary kriging utilize here is given below. Let $X_B = \{\boldsymbol{x}^1, \boldsymbol{x}^2, \ldots, \boldsymbol{x}^K\}$ denote a base set, such that the responses $\boldsymbol{R}(\boldsymbol{x}^j)$ of the EM antenna model are known for $j = 1, 2, \ldots, K$. Here, a simple design of experiments strategy is employed that iteratively generates random samples within the interval $[\boldsymbol{x}_{\min}, \boldsymbol{x}_{\max}]$ and accepts the ones that are within the model domain. The iterations are continued until the required number of samples has been found. It should be mentioned that this sampling technique also allows for estimating the ratio of the original (unconstrained) parameter space and the constrained surrogate model domain. For the examples considered in Section III, the ratio is a few orders of magnitude (from 10^4 to over 10^6). As mentioned before, this ratio primarily depends on $d_{\max}$ and the value of the latter should be adjusted to keep it at the aforementioned level; $d_{\max} = 0.1$ seems to be a reasonable starting value.

Let $\boldsymbol{R}(\boldsymbol{x}) = [R_1(\boldsymbol{x}) \ldots R_m(\boldsymbol{x})]^T$, where components of the model response are evaluations of the antenna responses of interest (here, reflection coefficient) at m frequency points. Ordinary kriging estimates deterministic function f as $f_p(\boldsymbol{x}) = \mu + \varepsilon(\boldsymbol{x})$, where μ is the mean of the response at the training points, and ε is the error with zero expected value, and with a correlation structure being a function of a generalized distance between the base points. We use a Gaussian correlation function of the form

$$Q(\boldsymbol{x}^i, \boldsymbol{x}^j) = \exp\left[\sum_{k=1}^{n} \theta_k \,|\, x_k^i - x_k^j \,|^2\right] \tag{7}$$

where θ_k are correlation parameters used to fit the model, while x_k^i and x_k^j are the kth components of the base points $\boldsymbol{x}^i$ and $\boldsymbol{x}^j$.

The kriging-based model $\boldsymbol{R}^{KR}$ is defined as

$$\boldsymbol{R}^{KR}(\boldsymbol{x}) = \left[R_1^{KR}(\boldsymbol{x}) \;\; \ldots \;\; R_m^{KR}(\boldsymbol{x})\right]^T \tag{8}$$

where

$$R_j^{KR}(\boldsymbol{x}) = \mu_j + \boldsymbol{r}^T(\boldsymbol{x})\boldsymbol{Q}^{-1}(\boldsymbol{f}_j - \boldsymbol{1}\mu_j) \tag{9}$$

Here $\boldsymbol{1}$ denotes an N-vector of ones,

$$\boldsymbol{f}_j = [R_j(\boldsymbol{x}^1) \;\ldots\; \ldots R_j(\boldsymbol{x}^K)]^T \tag{10}$$

$\boldsymbol{r}$ is the correlation vector between the point $\boldsymbol{x}$ and base points

$$\boldsymbol{r}^T(\boldsymbol{x}) = [Q(\boldsymbol{x}, \boldsymbol{x}^1) \;\ldots\; \ldots Q(\boldsymbol{x}, \boldsymbol{x}^K)]^T \tag{11}$$

whereas $\boldsymbol{Q} = [Q(\boldsymbol{x}^j, \boldsymbol{x}^k)]_{j,k = 1,\ldots,K}$ is the correlation matrix. The mean μ_j is given by $\mu_j = (\boldsymbol{1}^T\boldsymbol{Q}^{-1}\boldsymbol{1})^{-1}\boldsymbol{1}^T\boldsymbol{Q}^{-1}\boldsymbol{f}_j$. Correlation parameters θ_k are found by maximixing $-[K\ln(\sigma_j^2) + \ln|\boldsymbol{Q}|]/2$ in which the variance $\sigma_j^2 = (\boldsymbol{f}_j - \boldsymbol{1}\mu_j)^T\boldsymbol{Q}^{-1}(\boldsymbol{f}_j - \boldsymbol{1}\mu_j)/K$ and $|\boldsymbol{Q}|$ are both functions of θ_k.

III. Illustration Examples

In this section, we discuss several examples illustrating the operation and performance of the proposed modeling methodology. Three antenna structures are considered, a UWB monopole, a uniplanar dual-band dipole, and a dual-band microstrip patch antenna.

A. Example 1: UWB Monopole

Our first example is an ultra-wideband monopole antenna shown in Fig. 4. The structure consists of a rectangular radiator with elliptical corner cuts as well as stepped-impedance feed line. The antenna is implemented on a 0.76-mm-thick substrate. The design parameters are $\boldsymbol{x} = [L_g\, L_1\, L_2\, W_1\, L_p\, W_p\, a\, b]^T$ (all dimensions in mm). The feeding line width W_0 is adjusted for a given substrate permittivity to ensure 50 ohm input impedance. The EM antenna model $\boldsymbol{R}$ is implemented in CST Microwave Studio [8] (~900,000 mesh cells, simulation time 2 minutes). The model includes the SMA connector to ensure reliability of antenna evaluation.

The objective is to construct a surrogate model of the antenna input characteristic assuming various dielectric permittivities ε_r of the substrate. The reference designs are optimized for minimum in-band reflection at $\varepsilon_r = 1.8, 3.0, 4.5$, and 6.0. We have $\boldsymbol{x}^{(1)} = [9.86\ 4.17\ 6.46\ 2.08\ 21.1\ 29.7\ 0.52\ 0.44]^T$, $\boldsymbol{x}^{(2)} = [9.45\ 4.02\ 6.33\ 1.41\ 19.9\ 26.7\ 0.57\ 0.41]^T$, $\boldsymbol{x}^{(3)} = [9.17\ 3.54\ 6.55\ 1.26\ 19.6\ 26.8\ 0.58\ 0.39]^T$, and $\boldsymbol{x}^{(4)} = [9.91\ 5.04\ 5.91\ 1.05\ 18.5\ 24.9\ 0.62\ 0.38]^T$. Based on these designs, the lower and upper bounds for design variables are established as $\boldsymbol{l} = [8.5\ 3.0\ 5.5\ 1.0\ 18.0\ 24.0\ 0.5\ 0.35]^T$, and $\boldsymbol{u} = [10.0\ 5.5\ 7.0\ 2.5\ 22.0\ 30.0\ 0.65\ 0.45]^T$. In this case, the triangulation of the reference design yields three simplexes (intervals): $\{\boldsymbol{x}^{(1)}, \boldsymbol{x}^{(2)}\}$, $\{\boldsymbol{x}^{(2)}, \boldsymbol{x}^{(3)}\}$, and $\{\boldsymbol{x}^{(3)}, \boldsymbol{x}^{(4)}\}$. For the sake of computational efficiency, the reference design have been optimized using trust-region gradient search with variable-fidelity EM simulation models, following the methodology of [30]. The optimization criteria was allocation of the antenna resonances at the required operating frequencies and maximization of the fractional bandwidths.

The proposed constrained sampling technique has been verified for $d_{\max} = 0.15$ by setting up the kriging interpolation surrogate model with 100, 200, 400, 800, and 1600 random samples. Figure 5 shows selected two-dimensional projections of the constrained sampling.

For the sake of verification, 100 independent test points were allocated in the model domain and the average relative RMS errors have been calculated. For comparison, the conventional kriging model was also constructed using training sets of the same sizes, allocated in the unconstrained domain determined by the aforementioned bounds $\boldsymbol{l}$ and $\boldsymbol{u}$. The errors have been reported in Table I. Note that the error level for conventional models (unconstrained sampling) is very high, i.e., it is not possible to obtain an acceptable prediction power due to design space dimensionality and parameter ranges. On the other hand, the constrained model ensures good accuracy, which is below 10 percent for 400 and more training samples. Figure 6 shows the surrogate and EM model responses at the selected test designs. Figure 7 shows comparison of conventional kriging surrogate (in an unconstrained space) and EM model responses for selected

MOST WIEDZY Downloaded from mostwiedzy.pl

0018-926X (c) 2018 IEEE. Personal use is permitted, but republication/redistribution requires IEEE permission. See http://www.ieee.org/publications_standards/publications/rights/index.html for more information.

This article has been accepted for publication in a future issue of this journal, but has not been fully edited. Content may change prior to final publication. Citation information: DOI 10.1109/TAP.2018.2839759, IEEE Transactions on Antennas and Propagation

test points. It is clear, that the quality of the conventional model is indeed very poor.

As an application, the antenna of Fig. 4 has been optimized for various values of substrate permittivity (2.2, 3.5, 4.3 and 5.6) using the surrogate established in the constrained domain. Comparison of the surrogate and EM-simulated responses of the optimized antenna are shown in Fig. 8.

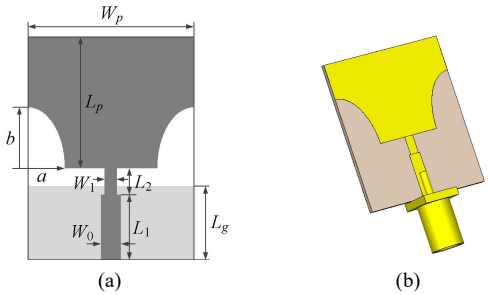

Fig. 4. Geometry of the planar UWB antenna: (a) top view, (b) 3D view. The ground plane marked with light-gray shade.

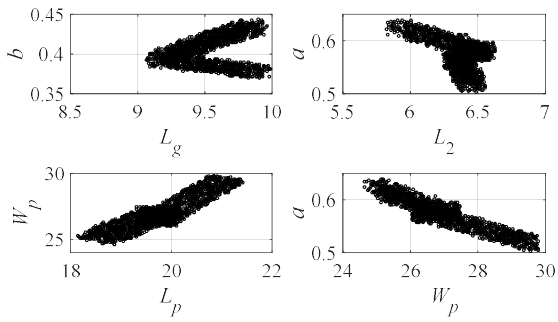

Fig. 5. Constrained sampling for selected two-dimensional projections onto L_g-b plane, L_2–a plane, L_p-W_p plane, and W_p-a plane.

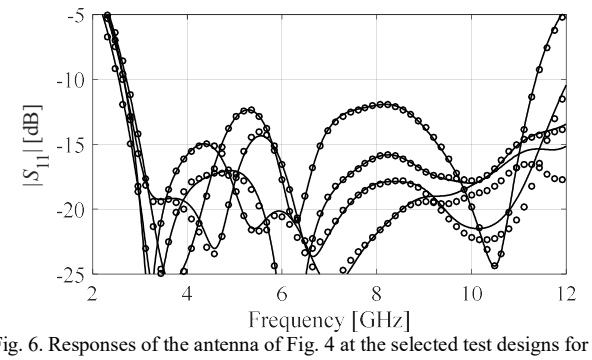

Fig. 6. Responses of the antenna of Fig. 4 at the selected test designs for N = 1600: high-fidelity EM model (—), proposed surrogate model (o).

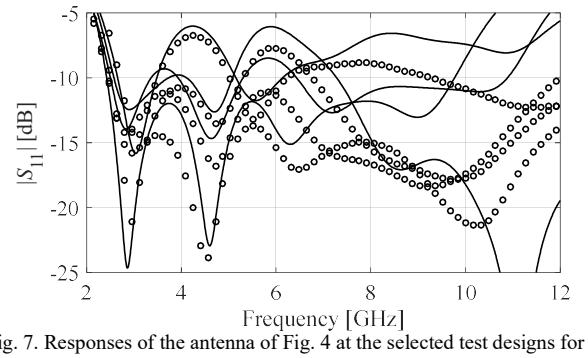

Fig. 7. Responses of the antenna of Fig. 4 at the selected test designs for N = 1600: high-fidelity EM model (—), conventional kriging surrogate (o).

Antenna designs for the two of the considered verification cases (ε_r = 2.2 and 3.5) have been fabricated and measured. For the first case, the TLP-5 substrate was used, for the second case, the antenna has been implemented on RF-35. Figure 9 shows the photographs of the antenna prototypes. The agreement between simulation and measurements is good as shown in Fig. 10.

Additional tests have been conducted in order to assess the effect of the model domain "thickness" controlled by the parameter $d_{\max}$. Clearly, it is expected that reducing the value of $d_{\max}$ would lead to improving the model predictive power because the domain will be reduced considerably. On the other hand, excessive reduction may result in inability of capturing the optimum antenna designs for the values of the figure(s) of interest (here, the substrate permittivity) that are allocated between those corresponding to the reference designs. Table II shows the modeling errors obtained for the constrained model and three values of $d_{\max}$: 0.2, 0.15 (used above), and 0.1. As expected, reducing the domain results in better prediction power. Now, in order to test the model applicability for design purposes, the verification designs have been optimized for the same values of permittivity as those listed in Fig. 8 (2.2, 3.5, 4.5, and 5.6). Figure 11 shows the comparison of selected designs for two values of $d_{\max}$, 0.1 and 0.2. It can be observed that lower $d_{\max}$ results, as expected (cf. Table II), in better agreement with EM simulation. On the other hand, the maximum in-band reflection of the optimized antenna is slightly better for higher $d_{\max}$ (because the model is valid over a larger region). However, the difference is minor (typically, a fraction of dB).

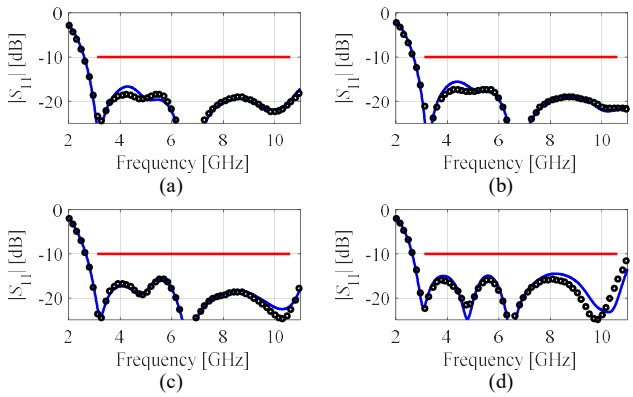

Fig. 8. Surrogate (o) and EM-simulated responses (—) of the antenna of Fig. 4 at the designs obtained by optimizing the proposed surrogate model for (a) ε = 2.2, (b) ε = 3.5, (c) ε = 4.3, and (d) ε = 5.6; –10 dB level for UWB frequency range marked using a horizontal line.

TABLE I MODELING RESULTS FOR EXAMPLE 1

Number of training samples#	Relative RMS Error*	
	Unconstrained sampling	Constrained sampling [this work]
100	68.3 %	15.1 %
200	68.9 %	11.6 %
400	68.5 %	10.0 %
800	67.8 %	9.9 %
1600	68.2 %	8.5 %

* In all cases, the surrogate model constructed using kriging interpolation.
\# The cost of finding the reference designs for constrained modeling is about 150 evaluations of the EM antenna model.

MOST WIEDZY Downloaded from mostwiedzy.pl

026X (c) 2018 IEEE. Personal use is permitted, but republication/redistribution requires IEEE permission. See http://www.ieee.org/publications_standards/publications/rights/index.html for more information.

This article has been accepted for publication in a future issue of this journal, but has not been fully edited. Content may change prior to final publication. Citation information: DOI 10.1109/TAP.2018.2839759, IEEE Transactions on Antennas and Propagation

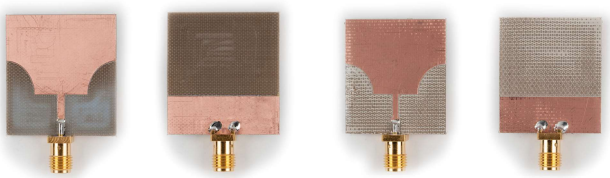

(a) (b)

Fig. 9. Photographs of the optimized antennas fabricated on (a) TLP-5 substrate ($\varepsilon_r = 2.2$), and RF-35 ($\varepsilon_r = 3.5$).

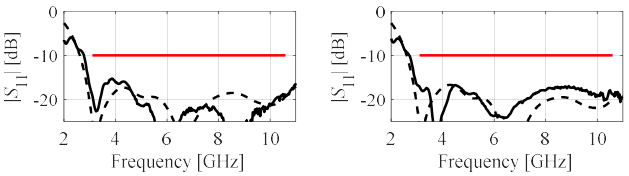

(a) (b)

Fig. 10. Reflection responses of the antennas of Fig. 9: (a) $\varepsilon_r = 2.2$, (b) $\varepsilon_r = 3.5$; simulation results (- - -) and measurements (—).

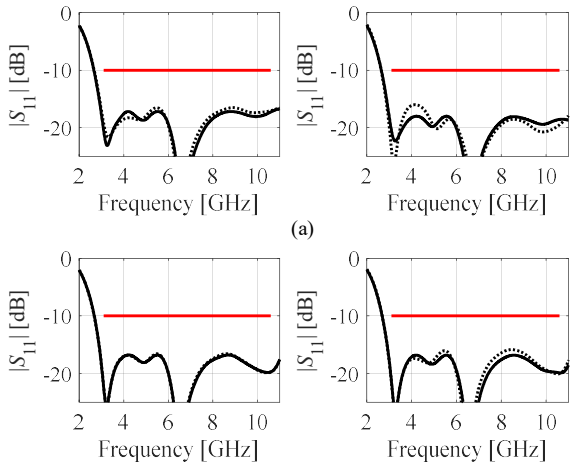

(a)

(b)

Fig. 11. Antenna of Fig. 4 at the designs obtained by optimizing the proposed surrogate model for (a) $\varepsilon = 3.5$, and (b) $\varepsilon = 5.6$; surrogate model response (—) versus EM model response (····). Left- and right-hand-side panels are for $d_{\max} =$ 0.1, and 0.2, respectively; –10 dB level for UWB frequency range marked using a horizontal line.

TABLE II MODELING RESULTS FOR EXAMPLE 1 FOR VARIOUS VALUES OF CONTROL PARAMETER d_{MAX}

Number of training samples	Relative RMS Error*		
	$d_{\max} = 0.2$	$d_{\max} = 0.15$	$d_{\max} = 0.1$
100	18.9 %	15.1 %	15.0 %
200	14.4 %	11.6 %	10.1 %
400	13.3 %	10.0 %	7.8 %
800	11.4 %	9.9 %	6.5 %
1600	9.7 %	8.5 %	5.8 %

B. *Example 2: Uniplanar Dipole Antenna*

The second example is a dual-band uniplanar dipole antenna shown in Fig. 12 [28]. The antenna is implemented on Taconic RF-35 ($\varepsilon_r = 3.5$, $\tan\delta = 0.0018$, $h = 0.762$ mm). The structure consists of two narrow ground plane slits interconnected through a thick slot. It is fed by a 50 Ohm coplanar waveguide (CPW). The variables are: $\boldsymbol{x} = [l_1\ l_2\ l_3\ w_1\ w_2\ w_3]^T$, whereas $l_0 = 30$, $w_0 = 3$, $s_0 = 0.15$ and $o = 5$ are fixed (all dimensions in mm). The EM antenna model $\boldsymbol{R}$ (~100,000 cells; 60 s simulation on a dual Xeon E5540 machine) is implemented in CST Studio [8].

We are interested in modeling the antenna for the following ranges of operating frequencies 2.0 GHz $\leq f_1 \leq$ 4.0 GHz (lower band), and 4.5 GHz $\leq f_2 \leq$ 6.5 GHz (upper band). There are 12 reference designs selected, corresponding to the antenna optimized for the pairs of operating frequencies as shown in Fig. 13. The lower and upper bounds for design variables were set using the reference designs as $\boldsymbol{l} = [25.0\ 6.0\ 14.0\ 0.2\ 1.6\ 0.5]^T$, and $\boldsymbol{u} = [35.0\ 15.0\ 21.0\ 0.55\ 4.0\ 2.0]^T$. For the sake of computational efficiency, the reference design have been obtained using feature-based optimization framework with variable-fidelity EM simulation models, following the methodology of [13]. The optimization criterion was reduction of the maximum in-band reflection within the UWB frequency range (3.1 GHz to 10.6 GHz).

The constrained sampling technique has been verified for $d_{\max} = 0.05$ by setting up the kriging interpolation surrogate model with 100, 200, 400, 800, and 1600 random samples. Figure 14 shows selected two-dimensional projections of the constrained sampling. The model accuracy has been verified using 100 independent test points. The average RMS errors for the constrained sampling and conventional kriging models have been reported in Table III. The error is defined as relative in the following sense: $\|\boldsymbol{R}(\boldsymbol{x}) - \boldsymbol{R}_{kr}(\boldsymbol{x})\|/\|\boldsymbol{R}(\boldsymbol{x})\|$. It can be observed that the constrained model exhibits much better accuracy than the conventional one. Figure 15 shows the surrogate and EM model responses at the selected test designs. Figure 16 shows a similar comparison for the conventional surrogate and the EM model, indicating inferior (compared to the constrained surrogate) performance.

To demonstrate the practical applications, the antenna of Fig. 12 has been optimized for several pairs of operating frequencies as indicated in Fig. 17. The same figure shows a comparison between the surrogate and EM model responses at the optimized designs.

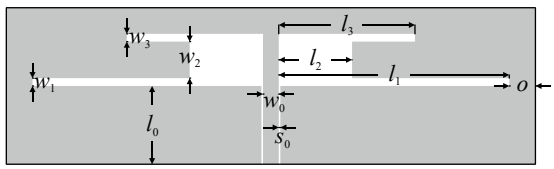

Fig. 12. Geometry of a dual-band uniplanar dipole antenna [26].

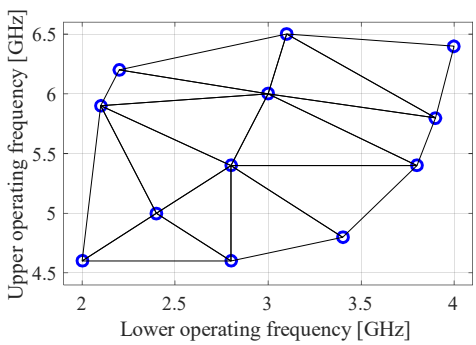

Fig. 13. Frequency allocation of the reference designs for the antenna of Fig. 11, and their triangulation.

MOST WIEDZY Downloaded from mostwiedzy.pl

026X (c) 2018 IEEE. Personal use is permitted, but republication/redistribution requires IEEE permission. See http://www.ieee.org/publications_standards/publications/rights/index.html for more information.

This article has been accepted for publication in a future issue of this journal, but has not been fully edited. Content may change prior to final publication. Citation information: DOI 10.1109/TAP.2018.2839759, IEEE Transactions on Antennas and Propagation

All verification designs have been fabricated and measured. Figure 18 shows the photographs of the antenna prototypes. Reflection responses shown in Fig. 19 indicate good agreement between simulation and measurements. Slight frequency shifts are mostly due to not including SMA connectors in the EM antenna model.

C. Example 3: Dual-Band Patch Antenna

Our last example is a dual-band planar antenna [29] shown in Fig. 20. The structure consists of two radiating elements in the form of a quasi-microstrip patch with inset feed and a monopole radiator. The antenna is implemented on a 0.762-mm-thick substrate. The design variables are $\boldsymbol{x} = [L\ l_1\ l_2\ l_3\ W\ w_1\ w_2\ g]^T$. The parameters $o = 7$, $l_0 = 10$ and $s = 0.5$ remain fixed. The feed line width w_0 is adjusted for a given substrate permittivity so as to ensure 50 ohm impedance. The unit for all dimensions is mm. The EM model is implemented in CST Microwave Studio [8]: (~400,000 mesh cells, simulation time 200 seconds).

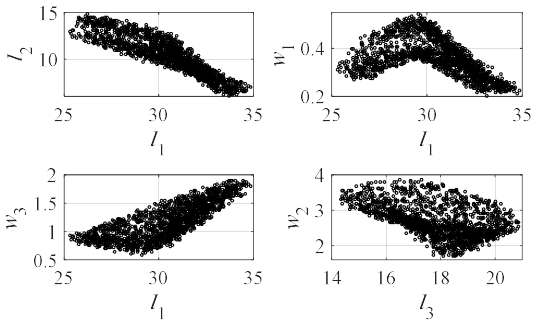

Fig. 14. Constrained sampling for selected two-dimensional projections onto l_1-l_2 plane, l_1–w_1 plane, l_1-w_3 plane, and l_3-w_2 plane.

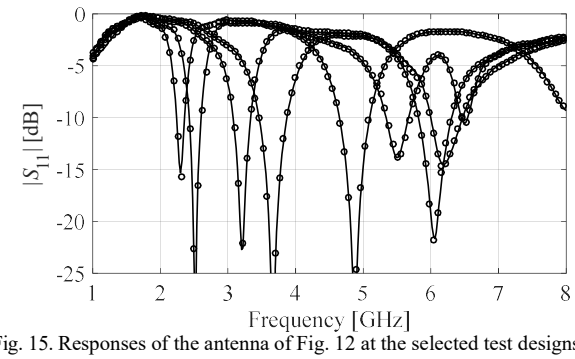

Fig. 15. Responses of the antenna of Fig. 12 at the selected test designs for N = 1600: high-fidelity EM model (—), proposed surrogate model (o).

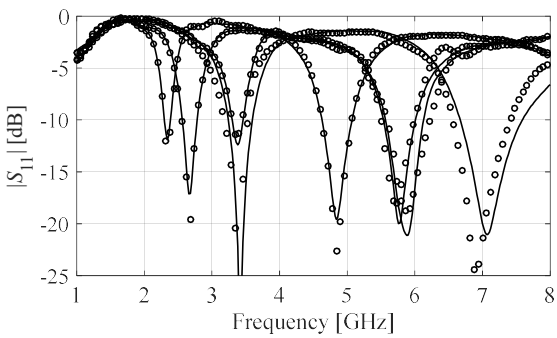

Fig. 16. Responses of the antenna of Fig. 12 at the selected test designs for N = 1600: high-fidelity EM model (—), conventional kriging surrogate (o).

We are interested in modeling the antenna for the following ranges of operating frequencies 2.0 GHz $\leq f_1 \leq$ 3.0 GHz (lower band), and 4.0 GHz $\leq f_2 \leq$ 6.0 GHz (upper band), and for substrate permittivity range $2.5 \leq \varepsilon_r \leq 5.0$. In this case, we prepare 20 reference designs as indicated in Fig. 21. All designs are optimized for corresponding operating frequencies and substrate permittivity. For the sake of computational efficiency, the reference design have been obtained using feature-based optimization framework with variable-fidelity EM simulation models, following the methodology of [13]. The optimization criteria was allocation of the antenna resonances at the required operating frequencies and maximization of the fractional bandwidths.

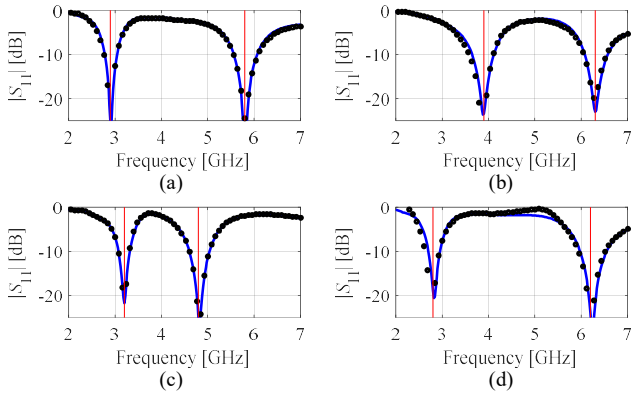

Fig. 17. Surrogate (o) and EM-simulated responses (—) of the antenna of Fig. 12 at the designs obtained by optimizing the proposed surrogate model for (a) f_1 = 2.9 GHz, f_2 = 5.8 GHz, (b) f_1 = 3.9 GHz, f_2 = 6.3 GHz, (c) f_1 = 3.2 GHz, f_2 = 4.8 GHz, and (d) f_1 = 2.8 GHz, f_2 = 6.2 GHz. Required operating frequencies are marked using vertical lines.

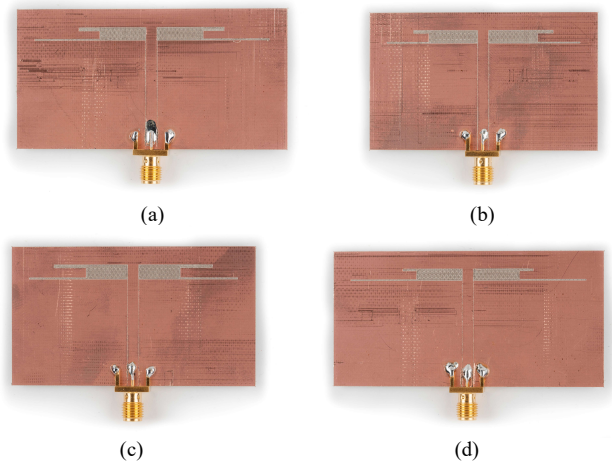

Fig. 18. Photographs of the optimized antennas: (a) f_1 = 2.9 GHz, f_2 = 5.8 GHz, (b) f_1 = 3.9 GHz, f_2 = 6.3 GHz, (c) f_1 = 3.2 GHz, f_2 = 4.8 GHz, and (d) f_1 = 2.8 GHz, f_2 = 6.2 GHz.

TABLE III MODELING RESULTS FOR EXAMPLE 2

Number of training samples#	Relative RMS Error*	
	Unconstrained sampling	Constrained sampling [this work]
100	17.2 %	4.6 %
200	12.7 %	3.5 %
400	9.3 %	2.8 %
800	6.9 %	2.6 %
1600	5.7 %	2.3 %

* In all cases, the surrogate model constructed using kriging interpolation.
\# The cost of finding the reference designs for constrained modeling is about 400 evaluations of the EM antenna model.

MOST WIEDZY Downloaded from mostwiedzy.pl

026X (c) 2018 IEEE. Personal use is permitted, but republication/redistribution requires IEEE permission. See http://www.ieee.org/publications_standards/publications/rights/index.html for more information.

This article has been accepted for publication in a future issue of this journal, but has not been fully edited. Content may change prior to final publication. Citation information: DOI 10.1109/TAP.2018.2839759, IEEE Transactions on Antennas and Propagation

The lower and upper bounds for design variables were set using the reference designs as $\boldsymbol{l}$ = [12 1.7 11 3.7 16.4 0.2 8.1 4.6]^T, and $\boldsymbol{u}$ = [24.5 4.5 12.3 9.4 18.3 2.2 9.8 6.6]^T.

The constrained sampling technique has been verified for $d_{\max}$ = 0.05 by setting up the kriging interpolation surrogate model with 100, 200, 400, 800, and 1600 random samples. Selected two-dimensional projections of the constrained set of training samples have been shown in Fig. 22. The model error (average relative RMS evaluated at 100 test points) are shown in Table IV for both the conventional and constrained surrogate.

The third example is the most complex one in terms of the number of design parameters and figures of merit taken into account in the modeling process. The conventional modeling strategy completely fails here (the modeling error at the level of 50% makes the model unusable even for 1600 training samples). The constrained modeling allows for obtaining decent accuracy as indicated in Fig. 23.

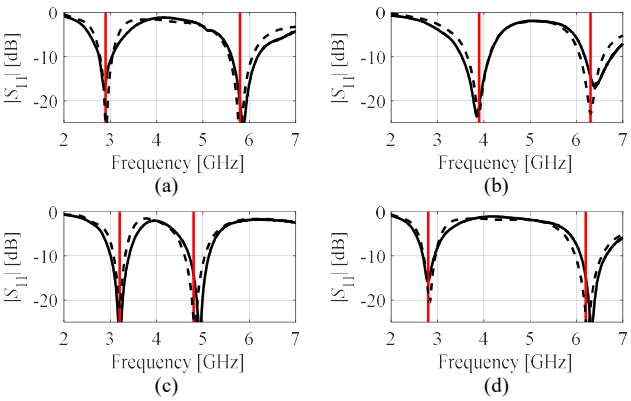

Fig. 19. Reflection responses of the antennas of Fig. 17: (a) f_1 = 2.9 GHz, f_2 = 5.8 GHz, (b) f_1 = 3.9 GHz, f_2 = 6.3 GHz, (c) f_1 = 3.2 GHz, f_2 = 4.8 GHz, and (d) f_1 = 2.8 GHz, f_2 = 6.2 GHz; simulation results (- - -) and measurements (—).

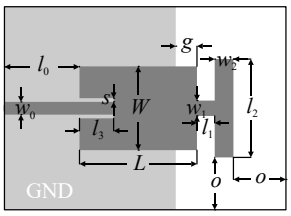

Fig. 20. Geometry of the dual-band patch antenna [18]. Ground plane marked using the lighter shade of gray.

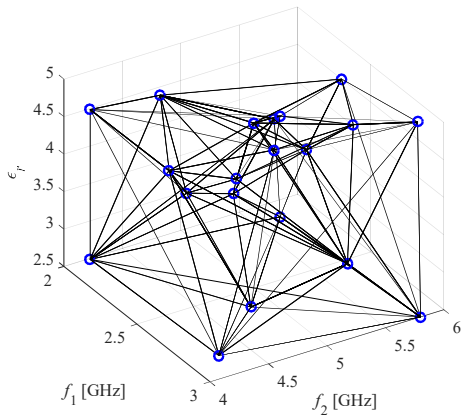

Fig. 21. Operating frequency (lower bound f_1 and upper band f_2) and substrate permittivity ε_r allocation of the reference designs for the antenna of Fig. 20, as well as their triangulation.

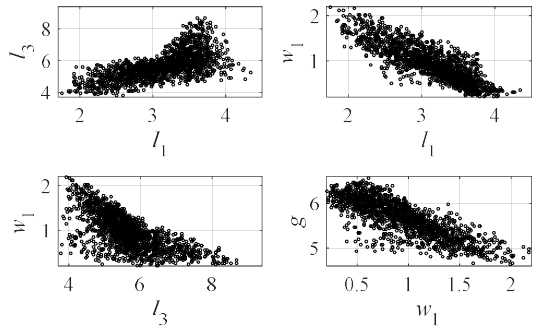

Fig. 22. Constrained sampling for selected two-dimensional projections onto l_1-l_3 plane, l_1–w_1 plane, l_3-w_1 plane, and w_3-g plane.

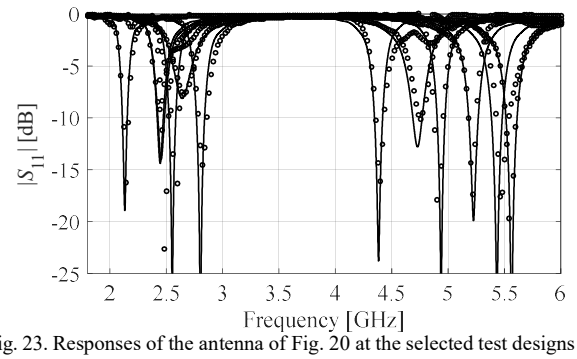

Fig. 23. Responses of the antenna of Fig. 20 at the selected test designs for N = 1600: high-fidelity EM model (—), proposed surrogate model (o).

TABLE IV MODELING RESULTS FOR EXAMPLE 3

Number of training samples#	Relative RMS Error*	
	Unconstrained sampling	Constrained sampling [this work]
100	50.5 %	19.1 %
200	49.1 %	16.5 %
400	48.8 %	14.6 %
800	48.9 %	12.9 %
1600	49.0 %	11.9 %

* In all cases, the surrogate model constructed using kriging interpolation.
\# The cost of finding the reference designs for constrained modeling is about 600 evaluations of the EM antenna model.

IV. CONCLUSION

In this work, a novel methodology for design-oriented surrogate modeling of antenna structures has been proposed. The key concept behind our approach is a definition of the surrogate model domain, spanned by a set of reference designs optimized for selected values of figures of interest such as operating frequencies of material parameters of the substrate. The geometrical structure of the model domain involves simplexes created by triangulating the reference designs. Mathematical formulation of the domain allows for arbitrary number and allocation of the reference designs (thus allowing us to reuse already existing designs if available). Comprehensive numerical validation involving three antenna structures of various types demonstrates that the presented methodology allows for considerable reduction of the number of training samples necessary to create the model of acceptable accuracy. The surrogate models have also been demonstrated using application studies (antenna optimization) with selected designs fabricated and measured for additional validation.

MOST WIEDZY Downloaded from mostwiedzy.pl

026X (c) 2018 IEEE. Personal use is permitted, but republication/redistribution requires IEEE permission. See http://www.ieee.org/publications_standards/publications/rights/index.html for more information.

This article has been accepted for publication in a future issue of this journal, but has not been fully edited. Content may change prior to final publication. Citation information: DOI 10.1109/TAP.2018.2839759, IEEE Transactions on Antennas and Propagation

It should be emphasized that the complexity of our design cases in terms of the number and range of geometry/material parameters as well as range of operating conditions considered is far beyond the cases normally considered in the literature in the surrogate modeling context. The future work will be focused on development of better design of experiments strategy in order to further improve the surrogate model reliability.

ACKNOWLEDGEMENT

The authors would like to thank Computer Simulation Technology AG, Darmstadt, Germany, for making CST Microwave Studio available.

REFERENCES

[1] J. Nocedal and S. Wright, *Numerical Optimization*, 2nd edition, Springer, New York, 2006.

[2] A.R. Conn, K. Scheinberg, and L.N. Vicente, *Introduction to Derivative-Free Optimization*, MPS-SIAM Series on Optimization, MPS-SIAM, 2009.

[3] M. Fernandez Pantoja, A. Rubio Bretones, and R. Gomez Martin, "Benchmark antenna problems for evolutionary optimization algorithms," *IEEE Trans. Ant. Prop.*, vol. 55, no. 4, pp. 1111-1121, 2007.

[4] S. Chamaani, M.S. Abrishamian, S.A. Mirtaheri, "Time-domain design of UWB Vivaldi antenna array using multiobjective particle swarm optimization," *IEEE Ant. Wireless Prop. Lett.*, vol. 9, pp. 666-669, 2010.

[5] J.I. Toivanen, J. Rahola, R.A.E. Makinen, S. Jarvenpaa, and P. Yla-Oijala, "Gradient-based antenna shape optimization using spline curves," *Annual Rev. Prog. Applied Comp. Electromagnetics*, Tampere, Finland, pp. 908-913, 2010.

[6] S. Koziel, F. Mosler, S. Reitzinger, and P. Thoma, "Robust microwave design optimization using adjoint sensitivity and trust regions," *Int. J. RF and Microwave CAE*, vol. 22, no. 1, pp. 10-19, 2012.

[7] M. Ghassemi, M. Bakr, and N. Sangary, "Antenna design exploiting adjoint sensitivity-based geometry evolution," *IET Microwaves Ant. Prop.*, vol. 7, no. 4, pp. 268-276, 2013.

[8] CST Microwave Studio, ver. 2016, CST AG, Bad Nauheimer Str. 19, D-64289 Darmstadt, Germany, 2016.

[9] Ansys HFSS, ver. 15.0 (2014), ANSYS, Inc., Southpointe 275 Technology Drive, Canonsburg, PA 15317.

[10] S. Koziel and S. Ogurtsov, "Antenna design by simulation-driven optimization. Surrogate-based approach," Springer, 2014.

[11] J. Zhu, J.W. Bandler, N.K. Nikolova and S. Koziel, "Antenna optimization through space mapping," *IEEE Trans. Ant. Prop.*, vol. 55, no. 3, pp. 651-658, March 2007.

[12] S. Koziel, S. Ogurtsov, and S. Szczepanski, "Rapid antenna design optimization using shape-preserving response prediction," *Bulletin of the Polish Academy of Sciences. Tech. Sc.*, vol. 60, no. 1, pp. 143-149, 2012.

[13] S. Koziel, "Fast simulation-driven antenna design using response-feature surrogates," *Int. J. RF & Microwave CAE*, vol. 25, no. 5, pp. 394-402, 2015.

[14] J.S. Ochoa, and A.C. Cangellaris, "Random-space dimensionality reduction for expedient yield estimation of passive microwave structures," *IEEE Trans. Microwave Theory Techn.*, vol. 61, no. 12, pp. 4313-4321, Dec. 2013.

[15] S. Koziel and J.W. Bandler, "Rapid yield estimation and optimization of microwave structures exploiting feature-based statistical analysis," *IEEE Trans. Microwave Theory Tech.*, vol. 63, no., 1, pp. 107-114, 2015.

[16] H.L. Abdel-Malek, A.S.O. Hassan, E.A. Soliman, S.A. Dakroury, "The ellipsoidal technique for design centering of microwave circuits exploiting space-mapping interpolating surrogates," *IEEE Trans. Microwave Theory Techn.*, vol. 54, no. 10, pp. 3731-3738, Oct. 2006.

[17] T.W. Simpson, J.D. Pelplinski, P.N. Koch, and J.K. Allen, "Metamodels for computer-based engineering design: survey and recommendations", *Engineering with Computers*, vol. 17, pp. 129-150, 2001.

[18] N.V. Queipo, R.T. Haftka, W. Shyy, T. Goel, R. Vaidynathan, and P.K. Tucker, "Surrogate-based analysis and optimization," *Progress in Aerospace Sciences*, vol. 41, no. 1, pp. 1-28, Jan. 2005.

[19] H. Kabir, Y. Wang, M. Yu, and Q.J. Zhang, "Neural network inverse modeling and applications to microwave filter design," *IEEE Trans. Microwave Theory Tech.*, vol. 56, no. 4, , pp. 867-879, April 2008.

[20] J. P. Jacobs and J. P. De Villiers, "Gaussian-process-regression-based design of ultrawide-band and dual-band CPW-fed slot antennas," *Journal of Electromagnetic Waves and Appl.,* vol. 24, pp. 1763-1772, 2010.

[21] A.J. Smola and B. Schölkopf, "A tutorial on support vector regression," *Statistics and Computing*, vol. 14, no. 3, pp. 199-222, Aug. 2004.

[22] G. Angiulli, M. Cacciola and M. Versaci, "Microwave devices and antennas modelling by support vector regression machines," *IEEE Trans. Magnetics*, vol. 43, pp. 1589-1592, 2007.

[23] J.L. Chavez-Hurtado, and J.E. Rayas-Sanchez, "Polynomial-based surrogate modeling of RF and microwave circuits in frequency domain exploiting the multinomial theorem," *IEEE Trans. Microwave Theory Tech.*, vol. 64, no. 12, pp. 4371-4381, 2016.

[24] I. Couckuyt, "Forward and inverse surrogate modeling of computationally expensive problems," Ph.D. Thesis, Ghent University, 2013.

[25] S. Koziel, "Low-cost data-driven surrogate modeling of antenna structures by constrained sampling," *IEEE Ant. Wireless Prop. Lett.*, vol. 16, pp. 461-464, 2017.

[26] S. Koziel, A. Bekasiewicz, "On reduced-cost design-oriented constrained surrogate modeling of antenna structures," *IEEE Ant. Wireless Prop. Lett.*, vol. 16, pp. 1618-1621, 2017.

[27] H. Borouchaki, P.L. George, and S.H. Lo, "Optimal Delaunay point insertion," *Int. J. Numerical Methods in Engineering*, vol. 39, no. 20, pp. 3407-3437, 1996.

[28] Y.-C. Chen, S.-Y. Chen, and P. Hsu, "Dual-band slot dipole antenna fed by a coplanar waveguide," *IEEE Int. Symp. Ant. Prop.*, pp. 3589-3592, 2006.

[29] S. Koziel, A. Bekasiewicz, and L. Leifsson, „Rapid EM-driven antenna dimension scaling through inverse modeling," *IEEE Antennas Wireless Prop. Lett.*, vol. 15, pp. 714-717, 2016.

[30] A. Bekasiewicz, and S. Koziel, "Structure and computationally-efficient simulation-driven design of compact UWB monopole antenna," *IEEE Antennas and Wireless Prop. Lett.*, vol. 14, pp. 1282-1285, 2015.

[31] Q.S. Cheng, S. Koziel, and J.W. Bandler, "Simplified space mapping approach to enhancement of microwave device models," *Int. J. RF and Microwave Computer-Aided Eng.*, vol. 16, no. 5, pp. 518-535, 2006.

Slawomir Koziel received the M.Sc. and Ph.D. degrees in electronic engineering from Gdansk University of Technology, Poland, in 1995 and 2000, respectively. He also received the M.Sc. degrees in theoretical physics and in mathematics, in 2000 and 2002, respectively, as well as the PhD in mathematics in 2003, from the University of Gdansk, Poland. He is currently a Professor with the School of Science and Engineering, Reykjavik University, Iceland. His research interests include CAD and modeling of microwave and antenna structures, simulation-driven design, surrogate-based optimization, space mapping, circuit theory, analog signal processing, evolutionary computation and numerical analysis.

Ari Thorlacius received his B.Sc. degree in mechatronics engineering from Reykjavik University, Iceland, in 2017. He is currently a research assistant at the Engineering Optimization & Modeling Center at Reykjavik University. His research interests include modeling and optimization of microwave and antenna structures, simulation-driven and computer-aided design, surrogate-based optimization, space mapping and numerical analysis.

MOST WIEDZY Downloaded from mostwiedzy.pl

026X (c) 2018 IEEE. Personal use is permitted, but republication/redistribution requires IEEE permission. See http://www.ieee.org/publications_standards/publications/rights/index.html for more information.